

# The radial metallicity gradient in the Galactic disk

Author: M<sup>a</sup>Carme Pujol Marín.

Advisors: Francesca Figueras Siñol and Maria Monguió i Montells.

*Facultat de Física, Universitat de Barcelona, Diagonal 645, 08028 Barcelona, Spain.*

(Dated: June 16, 2014)

**Abstract:** The aim of this work is to estimate the radial metallicity gradient in the Galactic disk toward the anticenter direction. For that we use Strömgren photometric data which allow us to compute individual physical parameters through empirical calibrations. We detect that metallicity calibrations found in the literature present discontinuities between photometric regions. By this, in the present work we focused in region 4, that is F0-G2 stars. Even though we detect some critical classification errors when faint stars are treated, induced by its larger observational uncertainties. To account for that, here we propose to use additionally the infra-red 2MASS photometry to clean the sample. We confirm that the metallicity gradient exists and decreases as we move away from the Galactic center. Our slope ( $d[Fe/H]/dR = -0.16 \pm 0.06 \frac{dex}{kpc}$ ) is slightly larger than recent results using APOGEE spectroscopic data.

## I. INTRODUCTION

The Milky Way is an excellent framework that provides the opportunity to measure large numbers of stellar abundances on a star-by-star basis. Observations of chemical abundances and derivations of metallicity gradients are very important for the understanding of the evolution and chemical structure of the Galactic disk.

The Apache Point Observatory Galactic Evolution Experiment (APOGEE) of the Sloan Digital Sky Survey-III is a high resolution near-infrared spectroscopic study that covers all the major components of the Galaxy. Recently Bovy et al. (2014)[1] with red-clump stars from APOGEE detected a quite steep metallicity gradient ( $d[Fe/H]/dR = -0.09 \pm 0.01 \frac{dex}{kpc}$ ). Moreover, the work of Hayden et al. (2014)[2] showed the existence of a negative radial metallicity gradient as a function of Galactic distance ( $d[M/H]/dR = -0.15 \pm 0.01 \frac{dex}{kpc}$  ( $9 < R < 11$ )).

On the other hand, Stinson et al. (2013)[3] analyzed the structure and chemical enrichment using simulated Milky Way-like galaxy. They found a correlation between metallicity, Galactic distance and age: the old stars have low metallicities and are far from the galactic center, while young stars are a short distance. Then, the fraction of stars with low metallicity increases at the outer parts of the disk, explaining the observed metallicity gradient.

In the present work, we aim to estimate the metallicity gradient through the Galactic anticenter direction. To achieve this, we use Strömgren photometric data from Monguió et al. (2013)[4] obtained with the Wide Field Camera at the Isaac Newton Telescope (Canary Islands). It is a photometric survey covering  $16^\circ$  in the anticenter direction with 96980 stars. 80% of them have spectral types later than A3 and are of interest of our purpose. This catalog provides a large number of stars for which we can compute its physical parameters -including metallicity- from empirical calibrations. We test the consistency and validity of some empirical calibrations in metallicity.

Hence, the present work is organized as follows: In the section II, we discuss the metallicity indicators in the Strömgren photometry, the photometric classification in regions and the empirical calibrations used. In the section III, we analyze and select our working sample, avoiding possible biases. In the section IV, we discuss the results of the radial metallicity gradient.

## II. STRÖMGREN PHOTOMETRIC SYSTEM

The Strömgren photometric system is widely used to determinate physical parameters for individual stars. It is an intermediate-band system designed to measure the Balmer discontinuity and the blanketing with the use of six filters:  $u, v, b, y, \beta_{wide}$  and  $\beta_{narrow}$ . With this filters we can define several magnitudes and indexes:

◊ The apparent visual magnitude,  $V$ , measured with the  $y$  filter.

◊ The  $(b - y)$  color index is used to determine effective temperature and the interstellar reddening.

◊ The  $m_1 = (v - b) - (b - y)$  index, is designed to measure the blanketing in the  $4100\text{\AA}$  with respect to a gradient defined by the  $b$  and  $y$  regions. Some empirical calibrations relate the  $m_1$  parameter and the metallicity  $[Fe/H]$  abundances.

◊ The  $c_1 = (u - v) - (v - b)$  index is designed to measure the Balmer discontinuity and measure temperature (intrinsic color) for B-type stars, and absolute magnitude (surface gravity) for A and F-type stars.

◊ The  $\beta = \beta_{narrow} - \beta_{wide}$  index measures the strength of the  $H\beta$  line in a spectrum of the star. It is a reddening-free index, since both filters (wide and narrow) are centered at the same wavelength. This parameter is correlated with the effective temperature, and it is unaffected by blanketing.

Crawford (1975)[5] defined the  $\delta m_1$  and  $\delta c_1$  indexes ( $\delta m_1 = m_1(\text{standard}) - m_1(\text{star})$  and  $\delta c_1 = c_1(\text{star}) - c_1(\text{ZAMS})$ ), where the values can be found in his table I. There are useful to take into account the chemical composition and evolution. Also, the relations between color

excesses allow us to define reddening free photometric indexes:  $[m_1] = m_1 + 0.33(b - y)$  and  $[c_1] = c_1 - 0.19(b - y)$ . Note that observed indexes have the suffix 1 and the intrinsic indexes have the suffix 0.

### A. Classification into photometric regions

The empirical calibrations relate the photometric indexes with physical parameters (intrinsic colors, absolute magnitude or metallicity). They are only valid for specific regions of the HR diagram. Thus we need to classify the stars in five photometric regions.

We use the Figueras et al. (1991)[6] criterion, that uses a free photometric indexes to classify in early group (region 1: B0-B9. 2), intermediate group (region 2: A0-A3) and late group: (i) region 3: A3 – F0; (ii) region 4: F0 – G2; region 5: G2 >.

In our study we are interested in the late group, since stars earlier than A3 the effects of variation in the metallicity are not appreciably in the photometric indexes. To distinguish between regions 3,4 and 5 we only use the  $\beta$  index as a temperature indicator[5]: region 3 ( $\beta > 2.72$ ), region 4 ( $2.58 < \beta < 2.72$ ) and region 5 ( $\beta < 2.58$ ).

### B. Empirical metallicity calibrations

Empirical metallicity calibrations have been established comparing photometric data with abundance obtained from spectroscopic analyses.  $[Fe/H]$  is the iron abundance of the star relative to the Sun:

$$[Fe/H] = \log_{10} \left( \frac{N_{Fe}}{N_H} \right)_* - \log_{10} \left( \frac{N_{Fe}}{N_H} \right)_{\odot}$$

The following calibrations are available from the literature:

◊ Olsen (1984)[10] proposed a second-order relation with the  $\delta m_0(\beta)$  index and  $c_0$ , valid for G0 – K1 dwarfs (region 5).

◊ Nissen (1987)[9] relate the  $[Fe/H]$  with  $\beta$  and  $\delta m_0(b - y)$  indexes, valid for main sequence stars in the range  $2.59 < \beta < 2.72$  (region 4). This relation was obtained using open clusters.

◊ Schuster and Nissen (1989)[8] proposed two different relations, for F-type and for G-type stars. The F-stars covered the ranges:  $0.22 \leq (b - y)_0 \leq 0.38$ ,  $0.03 \leq m_0 \leq 0.21$ ,  $0.17 \leq c_0 \leq 0.58$ . And for G-stars the calibration range was:  $0.37 \leq (b - y)_0 \leq 0.59$ ,  $0.03 \leq m_0 \leq 0.57$ ,  $0.10 \leq c_0 \leq 0.47$ . Hence, this calibration is only valid for region 4. Their relation is quite complex (including a logarithmic term) and uses  $m_0$  and  $(b - y)_0$  indexes. This calibrations has been obtained for high-velocity and metal-poor stars.

◊ Berthet (1990)[11] proposed a very general quadratic relation in terms of  $\delta m_0(\beta)$  based on a sample of 164 A – F main-sequence (MS) and giant stars. It is valid for  $\delta m_0 \geq -0.093$ .

◊ Smalley (1993)[7]. It is a linear relation with only the  $\delta m_0(\beta)$  index. It was obtained from 28 A and F-type stars, including several metal-rich Am-type stars. This calibration is valid for A3 – F0 stars with  $0.72 < \beta < 2.88$  (region 3).

◊ Haywood (2002)[13] defended that for F stars there was a mismatch between the standard sequence of the Hyades used by Schuster&Nissen and by Olsen in their photometric system. He proposed three different calibrations:  $0.22 < (b - y)_0 < 0.37$ ,  $0.37 < (b - y)_0 < 0.47$  and  $0.47 < (b - y)_0 < 0.59$ .

◊ Casagrande et al. (2011)[12] proposed a complex calibration using  $m_0$ ,  $(b - y)_0$  and  $c_0$ , valid for a large range:  $0.23 \leq (b - y)_0 \leq 0.63$ ,  $0.05 \leq m_0 \leq 0.68$ ,  $0.13 \leq c_0 \leq 0.60$ . Also, they proposed another calibration that performs significantly better for  $[Fe/H] \lesssim -1.0$ , arguing that Strömgren indexes lose sensitivity to low metallicities.

In Fig.1(a) we present an scheme of all these calibrations. As a first step, we have analysed their continuity when passing from one region to the next. That is when progressing in spectral type. We observed shifts in  $[Fe/H]$  of the order of 0.2-0.3 dex. So, a first warning appeared. That shift can be directly translated to a bias in the derivation of the radial metallicity gradient, the aim of this project. So, as a first step of this work we focus in region 4.

We found that the stars of our sample have a larger range than the standard relations ( $0.177 \leq m_0 \leq 0.226$ ) defined by Crawford (1975)[5] for the solar neighborhood. In Fig.1(b) and (c) we compare the analytical behaviors of metallicities calibrations in our range. Using Nissen calibration we can observe that for small  $\delta m_0$  values we obtain  $[Fe/H] > 1$  and this behavior is caused by the wrong extrapolation (spectroscopic data only shows values of  $[Fe/H]$  lowers for the solar neighborhood). In contrast, Berthet shows a good behavior in the hole range. The same can be applied to the calibration of Schuster&Nissen that reach unrealistic values up to  $[Fe/H] \approx 6$ . Haywood extrapolates better but also shows large values of metallicity and Casagrande calibration seems more well defined behavior.

## III. DATA AND SAMPLE SELECTION

### A. Our sample

We use the catalog from Monguió et al. 2013[4] that provides more than twenty thousand F0-G2 stars(56% of the catalog) towards the Galactic anticenter. As discussed, the catalog reach  $V \approx 18$  in the central part and contains stars with different photometric quality. Fig.2 estimates the distance coverage as a function of the apparent magnitude and the spectral type.

In order to define an accurate working sample we have followed the next criteria:

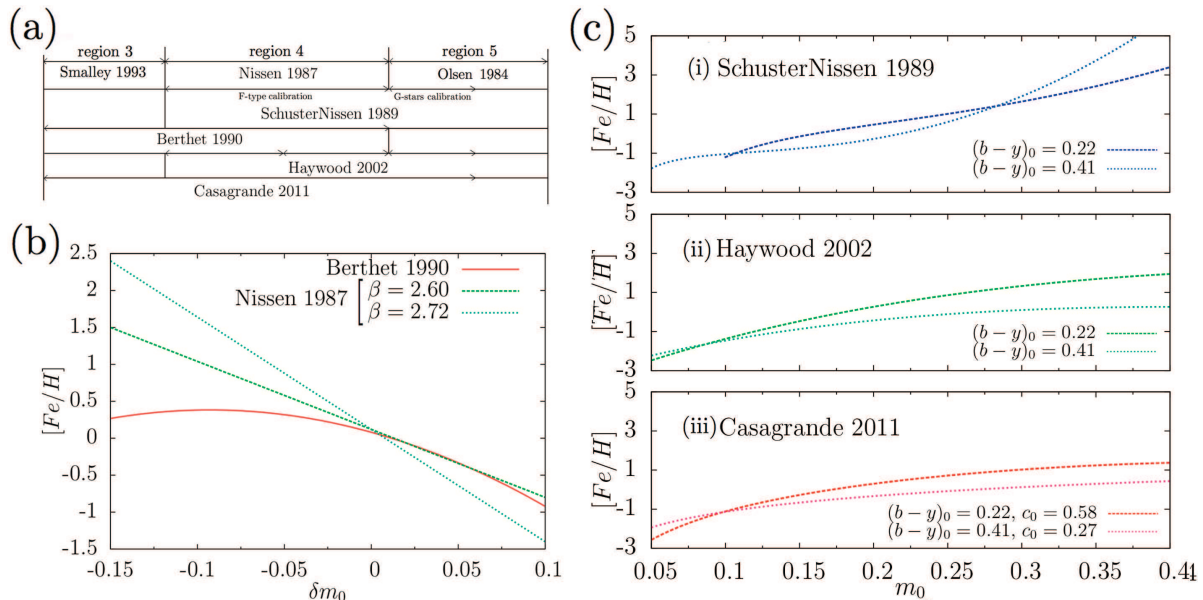


FIG. 1: (a) A schematic table with a validity ranges for all calibrations. (b) Berthet (continuous line) versus Nissen (dashed line) depending on  $\delta m_0$  index. For Nissen we give the limit values of  $\beta$  for the region 4. (c) Comparison of theoretical behavior of the different calibrations versus  $m_0$  index with a constant  $(b-y)_0$ . In (i) Schuster and Nissen calibration for F-type stars, in (ii) Haywood 2002 in the first range ( $0.22 \leq (b-y)_0 \leq 0.37$ ) and in (iii) the relation of Casagrande 2011.

(1) To avoid potential giants we refuse stars with  $\log g < 3.5$ . Where  $g$  is the surface gravity.

(2) To avoid possible contamination from OB-type stars we discard all the stars with  $[m_1] < 0.16$ .

(3) Some stars present a large absorption at a short distances. It is straightforward to see that it is incorrect. The problem could be related to extremely large observational errors in  $(b-y)$ , that cause large excess color values. For that, we refuse the stars that verify simultaneously:  $(b-y) > 1.0$  and  $\beta < 2.65$ .

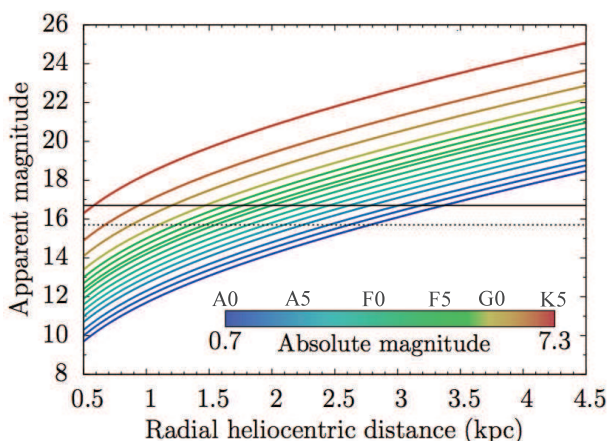


FIG. 2: Estimate of apparent limit magnitude ( $V$ ) as function of a distance for different absolute visual magnitude. We use an absorption of  $A_v \approx 1 \text{ mag/kpc}$ . The continuous black line shows the  $V_{lim} \approx 16.7$  (limit for inner region) and the dashed line shows the  $V_{lim} \approx 15.7$  (limit for outer region).

In Fig.3(a) we present the  $m_0$  histogram. When working with the full sample we observe an asymmetric distribution, having many more stars with high  $m_0$  values (high  $[Fe/H]$  abundances). This result is inconsistent with being  $F0-G2$  (possible classification problem). Observational errors in  $\beta$  may lead this miss classification.

We cross-matched our sample with the Two Micron All-Sky Survey (2MASS, Cutri et al. (2003)[4] catalog) providing  $JHK$  photometry. Absorption in these bands have been obtained through  $A_v$  and Rieke and Lebofsky (1985)[17] relations. That allow us to compute intrinsic 2MASS color indexes.

Fig.4 shows our  $F0-F9$   $V$  sample in the  $(J-K)_0$ ,  $(J-H)_0$  photometric diagram. We observe a lot of stars with color differences significantly larger than the tabulated values. Two possible explanations are: (i) we have a contamination of stars from region 5 classified as region 4 ( $\beta$  is overestimated) or (ii) we have underestimated color excess  $E(b-y)$ . A too large  $(b-y)_0$  coming of a too small  $\beta$ .

To clean the sample, we define:

◊ Sample A. Contains all stars after applying conditions (1)-(3).

◊ Sample B. We only use stars with more than two observation and with  $V < 15.7$ .

◊ Sample C. We reject stars with:  $0.04 \leq (J-H)_0 \leq 0.26$  and  $0.06 \leq (J-K)_0 \leq 0.33$ .

We show in Fig. 3  $m_0$  and  $\beta$  histograms for the samples. For the sample C the  $m_0$  histogram is more symmetrical and the  $\beta$  histogram shows a distribution more centered in the Crawford range than A and B samples.

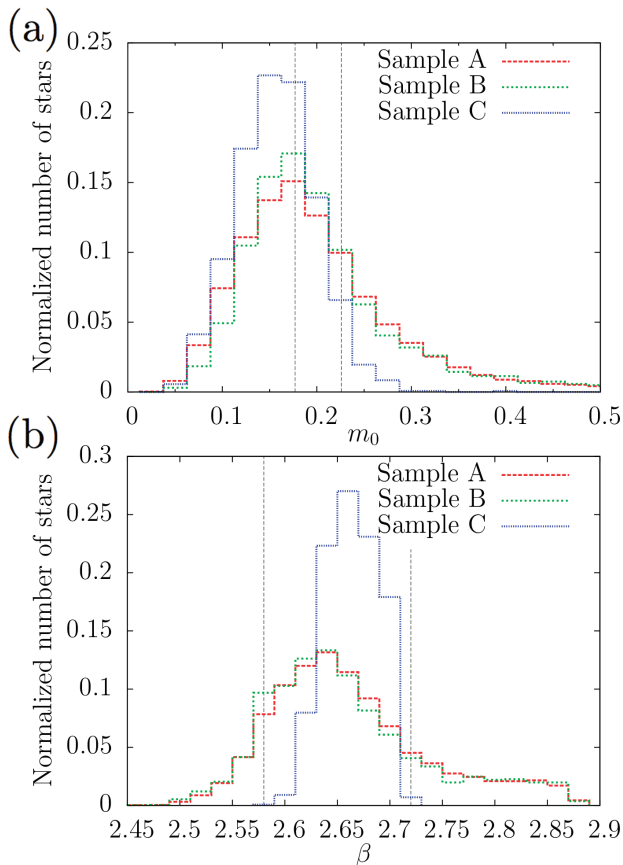


FIG. 3: Histograms of each sample for (a) metallicity indicator  $m_0$  and (b)  $\beta$  index. The dashed lines marks the edges of the standard relations[5].

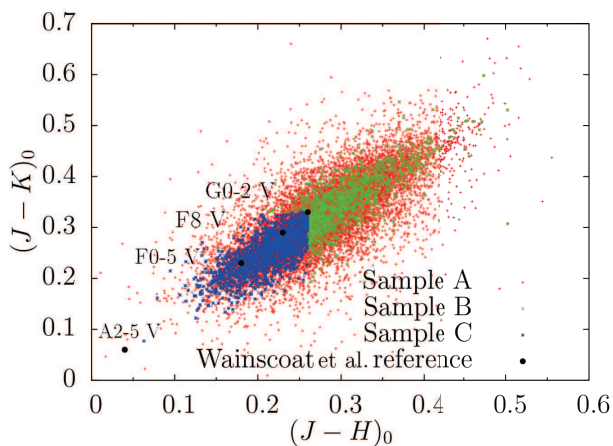


FIG. 4: We show the intrinsic color difference  $(J - K)_0$  versus  $(J - H)_0$  for the three samples. The black points are the tabulated values for Wainscoat (1992)[15]. The text labels corresponds to the spectral type of this points

## B. The derivation of the radial metallicity gradient

In order to calculate the gradient we use medians, because they are less influenced by outliers stars and show less dispersion in  $[Fe/H]$ . Other options have been tested, e.g. average discarding points greater than  $3\sigma$  and moving averages. But the first do not improve significantly the results using averages and the second option is greatly influenced by large distance points.

And for more consistency, we use the Galactic heliocentric distance  $(R - R_\odot)$ . The galactocentric distance is calculated for each of the stars as:  $R^2 = R_\odot^2 + (\rho \cdot \cos(b))^2 - 2R_\odot\rho \cos(b) \cos(l)$ . Where  $\rho$  is the radial heliocentric distance,  $l$  and  $b$  are the galactic longitude and latitude respectively.

## IV. RESULTS AND DISCUSSION

First, we take a Casagrande calibration to compare the behavior between the three samples, because are the more recent and extrapolate correctly (see section II. B). In Fig.5(a) we observe that  $[Fe/H]$  abundances decrease as we move away from the Galactic Center (GC). The values around 0.2–0.3 dex in the samples A and B can be a biased due to contamination of region 5 stars ( $> G2$ ). Note that median metallicity is similar to the solar, in a good agreement with Bovy et al. (2014)[1].

In Fig.5(b) we compare calibrations using the sample C. We observe that all the calibrations present the same behavior but with a different zero point. The calibration of Haywood do not improve the result from Schuster&Nissen calibration. Both give unrealistic values in short Galactic distances. In contrast, the Berthet and the Casagrande calibrations seem a well behavior. The differences with the type of stars used to build the calibrations (e.g. main sequence, giants, dwarfs or high velocity stars) can be related to their behavior differences. And also, observational uncertainties can produce discrepancies between results. Note that every calibration use different parameters and some of the relations are very complex.

The data can be fit by a single linear relation:  $[Fe/H] = -0.16 \pm 0.06 \frac{dex}{kpc} (R - R_\odot) + 0.06 \pm 0.05$  and  $[Fe/H] = -0.19 \pm 0.03 \frac{dex}{kpc} (R - R_\odot) + 0.16 \pm 0.03$  for Casagrande and for Berthet, respectively. This slopes are larger compared to the result given by Bovy et al. (2014)[1]. On the one hand, we have larger observational errors and difficulties in the classification into regions. We reduce significantly the number of stars to solve these problems increasing the statistical errors. On the other hand, the type of stars that we used to develop the study are different: they used a red-clump stars, while we use main sequence stars. We do not take into account the age of the stars while Bovy used stars with intermediate-age (1–5 Gyr old) that can be important since there was a relation between the metallicity and ages.



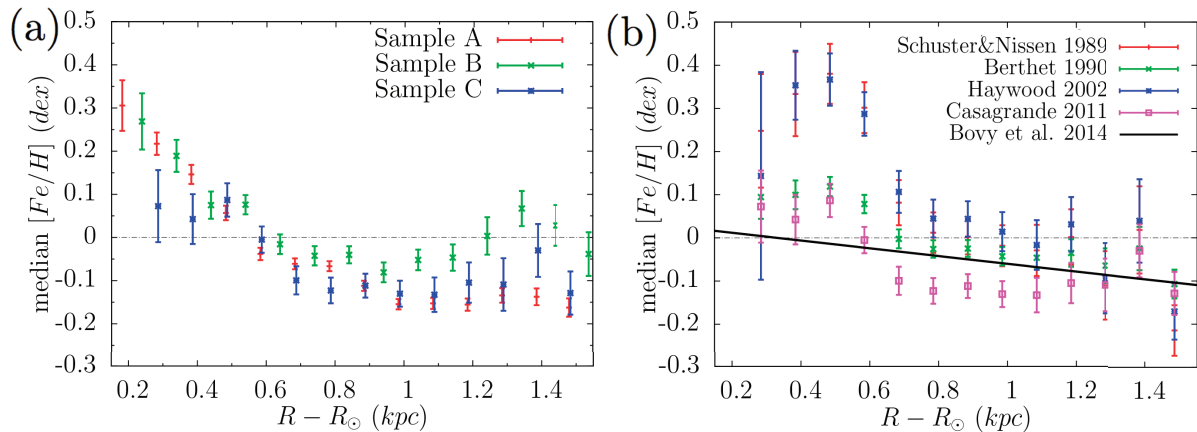


FIG. 5: We show  $[Fe/H]$  abundances versus the heliocentric distance. We observe a different behavior (a) depending on the sample. (b) depending on the calibration. The continuous line corresponds to the Bovy et al. 2014 [1] result.

## V. CONCLUSIONS AND NEXT STEPS

We have applied an empirical calibration method to estimate the radial metallicity gradient in the Galactic disk using Strömgren photometry. This method needs a previous classification into regions. This has been a challenge due to the large observational uncertainties in our photometric indexes for faint stars. That had led us to propose several strategies to clean the sample. We also compared different metallicity calibrations found in the literature showing the biases they introduce in the derivation of the metallicity gradient. Finally, we contrast our result with the work of Jovy et al. 2014 [1]. Our main results are:

- ◊ There is no good continuity between regions when deriving stellar metallicities.

- ◊ The calibrations of Nissen, Schuster&Nissen and Haywood show unrealistic values of metallicity (analytically and with our sample) in the edges of their intervals due to wrong extrapolation.

- ◊ The criteria of photometric classification into regions for faint stars are not enough to discriminate between region 4 ( $F0 - G2$ ) and 5 ( $> G2$ ). We propose to use 2MASS photometry to refuse possible contamination stars.

- ◊ Once this new criteria is applied, we check that the metallicity in the first radial bins is similar to the solar metallicity ( $\pm 0.1$  dex).

- ◊ We confirm that the radial gradient exist in the plane and decreases as we move away from the Galactic center.

- ◊ Our slope  $-0.16 \pm 0.06 \frac{dex}{kpc}$  is larger than the recent value of APOGEE.

The use of spectroscopic data may help us to calibrate the metallicity scale. The next step would be also to use regions 3 and 5 and find a more general relation valid for MS stars and introduce other type of stars as giants.

Let us hope that Gaia will provide us more accurate information to explain the structure, formation and evolution of our galaxy.

### Acknowledgments

First and foremost, I would like to thank my advisors, Francesca Figueras and Maria Monguió for all their help, dedication and patience, always looking for alternatives when the results were not as expected. I have much to learn from them. Also, thank my family and friends for always supporting me all previous years. Finally, a special thanks to Álvaro for always being by my side.

[1] Bovy, Jo, et al. *arXiv preprint:1405.1032* (2014).  
 [2] Hayden, Michael R., et al. *AJ* 147.5 (2014): 116.  
 [3] Stinson, G. S., et al. *MNRAS* 436.1 (2013): 625-634.  
 [4] Monguió, M., F. Figueras, and P. Grosbol. *VizieR Online Data Catalog* 354 (2012): 99078.  
 [5] Crawford, D. L. *AJ* 80 (1975): 955-971.  
 [6] Figueras, F., J. Torra, and C. Jordi. *A&AS* 87 (1991): 319-334.  
 [7] Smalley, B. *A&A* 274 (1993): 391.  
 [8] Schuster, W. J., and P. E. Nissen. *A&A* 221(1989):65-77.  
 [9] Nissen, P. E. *A&A* 199 (1988): 146-160.

[10] Olsen, E. H. *A&AS* 57 (1984): 443-466.  
 [11] Berthet, S. *A&A* 236 (1990): 440-448.  
 [12] Casagrande, L., et al. *arXiv preprint:1103.4651* (2011).  
 [13] Haywood, M. *MNRAS* 337.1 (2002): 151-160.  
 [14] 2MASS All-Sky Catalog of Point Sources (Cutri et al. 2003).  
 [15] Wainscoat, Richard J., et al. *A&AS* 83 (1992): 111-146.  
 [16] Monguió i Montells, Maria. PhD thesis. UB (2013).  
 [17] Rieke, G. H., and M. J. Lebofsky. *AJ* 288(1985):618-621.